ELSEVIER

Polymer 41 (2000) 733–741

polymer

Monomer functionality effects in the anisotropic phase separation of liquid crystals

R.T. Pogue[a,*], L.V. Natarajan[a], S.A. Siwecki[a], V.P. Tondiglia[a], R.L. Sutherland[a], T.J. Bunning[b]

[a]*Science Applications International Corporation, 4031 Colonel Glenn Hwy., Dayton, OH 45431, USA*
[b]*AFRL/MLPJ, Materials and Manufacturing Directorate, WPAFB, OH 45432, USA*

Received 1 December 1998; received in revised form 4 March 1999; accepted 8 March 1999

Abstract

Holographic gratings formed through the anisotropic phase separation of liquid crystals show promise as switchable optical elements. In order to form useful elements, however, it is necessary to control the nanoscale morphologies within the grating films. In this manuscript, we evaluate the role of monomer functionality on the morphology and the electro-optical properties of both gratings and conventional scattering polymer-dispersed liquid crystal (PDLC) films. Both of these structures are formed using polymerization-induced phase separation (PIPS) of liquid crystals from a cross-linked polymer formed through free-radical photo-polymerization. Floodlit (uniform illumination) films and holographic gratings (from non-uniform illumination caused by the interference of two laser beams) were made using monomers with 2–5 acrylate groups, while keeping the LC concentration constant in the syrups. The morphologies of these films were examined using low voltage scanning electron microscopy (LVSEM). In all cases, very small LC domains were formed with little indication of growth or coalescence. Lowering monomer functionality reduced the volume fraction of phase-separated domains in the floodlit samples. For the grating samples, the local volume fraction and the LC domain sizes decreased substantially as the monomer functionality was decreased. Using detailed image analysis, differences in the anisotropy of the domains was also probed. A much stronger tendency to form anisotropically-shaped domains was observed for the higher functional syrups. These domain anisotropy differences are correlated with the number of reactive double bonds per monomer and are suggestive of local environmental differences exerted at the time of the domain formation.

Keywords: Polymer-dispersed liquid crystal; Morphology; Grating

1. Introduction

Polymer-dispersed liquid crystals (PDLCs) [1] are being widely studied for use in a number of new electro-optic applications. This widespread interest results from the fact that PDLCs can be switched between a transparent and a scattering state by an AC electric field. The fact that polarizers are unnecessary allows high contrast switchable films to be formed. A number of preparation techniques have been examined including encapsulation techniques and thermally- and solvent-induced phase separations. The most widely used technique, however, is polymerization-induced phase separation (PIPS). This technique allows for a high degree of control over the final properties of the film. In this method, a low molecular weight liquid crystal (LC) is mixed with a reactive monomer and a polymerization initiator. The polymerization is then initiated either by heat or light and phase separation occurs as the molecular weight and cross-link density of the growing polymer chains increases. By controlling the polymerization rate, initial composition of components and/or processing temperature, a wide variety of morphologies have been generated ranging from discrete, spherical domains to a bicontinuous network of polymer fibrils and LC domains. This control of the film morphology is important as it serves to modulate the electro-optical properties of these films.

Most PDLC systems possess LC domains larger than a micron. This serves two purposes, first, the large size scale contributes to a large scattering cross-section and second, the large domains serve to lower the switching voltages. The second attribute is frequently cited as an important requirement in the transition of PDLC technology to commercial applications. Drzaic [1] has reviewed the effect of domain size on switching field and has shown that this field scales as $1/R$ where R is the average droplet radius observed in the

* Corresponding author. Tel.: +1-937-431-2220; fax: +1-937-431-2288.
E-mail address: robert.t.pogue@cpmx.saic.com (R.T. Pogue)

0032-3861/00/$ - see front matter
PII: S0032-3861(99)00196-2

film. It is important to emphasize that there is a distribution of droplet sizes within typical PDLC films and that the character of this distribution is related to the kinetics of the phase separation process. It can also be shown that the switching field is inversely proportional to droplet anisotropy.

For submicron droplets, both of these factors become especially important as stronger surface forces and director orientations are expected. For most systems studied to date, the size and shape of the droplets is assumed to be formed in a quasi-equilibrium state and thought to be formed by phase separation followed by growth of the domains. Most PDLC literature assumes that this morphology is fixed upon gelation of the matrix. The role of the surrounding polymer is typically not discussed as large droplets with a considerable volume/surface ratio are formed. However, several groups have investigated sub-micron droplets formed using PIPS-based processes [2–5]. These systems do not appreciably scatter light and their utility has been centered on making switchable retardation films. When the domain sizes become small enough, one can invoke effective medium theory allowing the film to be considered as possessing only a single refractive index. Application of an electric field allows one to vary the refractive index of these films. These films are formed by the rapid polymerization of free-radical monomers.

A number of groups have extended PDLC systems into a regime where one controls the spatial registry of the phase-separated structures [6–15]. The development of periodic arrays of PDLC droplets embedded in a polymeric matrix results in a refractive index profile across the film giving rise to diffraction of light. The ability to switch the effective refractive index of the LC domains results in the control of the diffraction of light from these structures. These structures can be formed on a variety of length scales ranging from the Raman–Nath regime (typical periodicity greater than 1.5 μm) to the Bragg regime (spacings less than 1.5 μm). Most of the work originating from our group [12–15] stems from the fabrication of Bragg transmission and reflection gratings which necessitates spatially periodic phase separated LC domains with spacings typically less than 1 μm. In order to prepare these PDLC gratings, the LC droplets must have diameters of less than half the grating spacing. Thus, phase separated structures with very small LC domains (<100 nm) are typically formed. Remarkably, these structures are, in general, still active electro-optically although switching performance is diminished as the domain sizes and distribution decrease. An electro-optic model to account for differences in the theoretical electro-optic performance has been successfully developed [16].

In order to form such small domains, highly functionalized monomers are employed resulting in films with high cross-link density. It is interesting to speculate that the nature of the polymer network (highly functionalized) employed coupled with the small domains formed and the anisotropic nature of the writing process might affect the nature of the phase-separated domains. Indeed, previous work by our group has shown that minor changes in the monomer functionality induced by the addition of a mono-functional monomer leads to large differences in the morphology of both HPDLC and standard PDLC samples [17,18]. Higher concentrations of a mono-functional monomer lead to decreased local LC volume fractions in the LC-rich regions and smaller LC domains on an average. Large differences in the degree of anisotropy of these domains was observed but not quantified.

Although the nature of our system ensures that we are not in a thermodynamic equilibrium condition and that kinetics play a huge factor in dictating behavior, it is interesting to compare these results to some previously published work. Kloosterboer and co-workers [19–21] have illustrated that the morphologies and optical properties of PDLCs of di- and mono-acrylate mixtures are dramatically affected by such factors as LC content, curing temperature, multiple exposures, and the presence of cross-linking agents. They showed that by increasing the amount of monofunctional acrylate in a prepolymer syrup, the conversion at phase separation was greatly increased. Furthermore, the observed domain sizes decreased with decreasing diacrylate concentration until the LC droplets were too small to study. They used this work to present a discussion on the concept of liquid–gel demixing as a mechanism for phase separation in certain concentration regimes. To this argument they add an elasticity term into the traditional Flory–Huggins theory of liquid–liquid demixing. Inclusion of this term is based on previous studies by Dusek et al. [22,23] in which the contributions of the cross-link density and gelation fraction are considered in the thermodynamics of phase separation. Most important, however, were the experimental results that indicated small, anisotropic droplets with an apparent lack of any coalescence were observed under the higher cross-link density condition. They [19–21] attribute these differences to changes in the local environment that the LC domains experience upon phase separation. Because the system has already gelled, the domains “feel” their surrounding environment due to a lack of host flexibility induced by the cross-links. Higher cross-linking leads to more elastic stresses and thus more misshapen droplets are observed. The strong networks also preclude any appreciable droplet growth and coalescence.

The observations of this past work were consistent with our previous work, although the length scales where considerably different. We continue our investigation of the diversity of morphologies induced by variation of the monomer by examining standard PDLC and HPDLC samples formed with monomers with different number of double bonds. All of these samples exhibit phase separation of very small LC domains (<100 nm). The nanostructure of these two-phase systems is investigated with low voltage scanning electron microscopy (LVSEM) and image analysis is used to explore differences in droplet size, shape and dispersity.

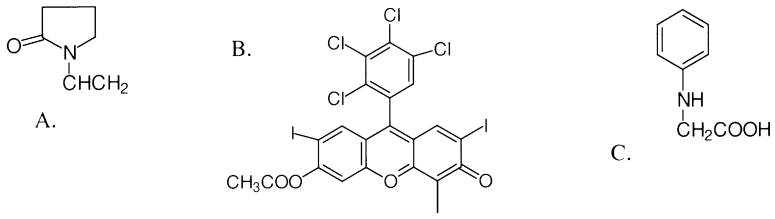

Fig. 1. Chemical structures of the solubilizing agent used in the syrup: *N*-vinyl pyrrolidone (NVP) (A); the co-initiator *N*-phenyl glycine (NPG) (B); and the photoinitiator, a Rose Bengal derivative (C).

2. Experimental

Chemical structures of the components used are given in Figs. 1 and 2. *N*-vinyl pyrrolidone (NVP) (A) and *N*-phenyl glycine (NPG) (B) were obtained from Aldrich and used as received. The photoinitiator, (RBAX), (C) was received from Spectragroup Limited and was used without purification. The monomers shown in Fig. 2 are all acrylate derivatives. Each possesses a different number of double bonds. Dipentaerythritol pentaacrylate (A); pentaerythritol tetraacrylate (B); pentaerythritol triacrylate (C); trimethylolpropane triacrylate (D); and tripropyleneglycol diacrylate (E) were obtained from Sartomer and used without further purification. Several of the higher functionality monomers are mixtures of various functionality derivatives. HPLC analysis of the mixtures was conducted to yield composite monomer functionalities that were calculated from the relative percentages. These values are shown in Table 1 and in general indicate that the average number of double bonds on the monomers decreased upon going from monomer A to monomer E. We assume that the double bonds on each monomer have the same inherent initial reactivity as double bonds on any other monomer. The similarity of the structures shown in Fig. 2 indicates that this is a reasonable assumption. The liquid crystal employed was E7 (EM Industries), a eutectic liquid crystal mixture consisting of three cyanobiphenyls and one cyanoterphenyl. All syrups contained the same amount of LC (33 wt.%), NVP, NPG and RBAX. Samples were prepared on cleaned glass or ITO-coated glass substrates.

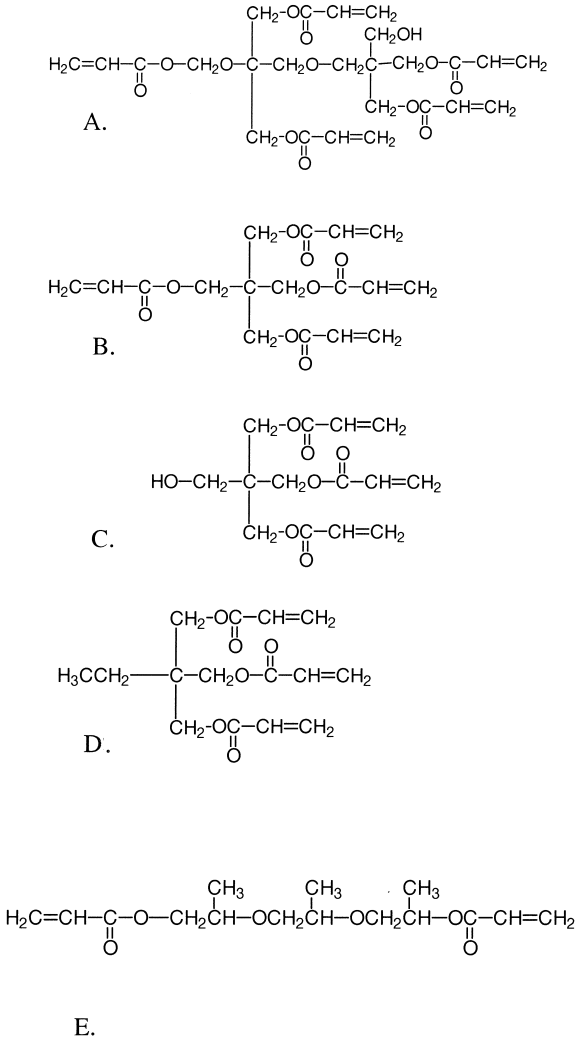

Fig. 2. Chemical structures of predominant monomers: dipentaerythritol pentaacrylate (A); pentaerythritol tetraacrylate (B); pentaerythritol triacrylate (C); trimethylolpropane triacrylate (D); and tripropyleneglycol diacrylate (E).

Syrups were placed between glass substrates using 15 μm spacers to control the thickness. Samples cured isotropically were illuminated with an Argon-ion laser at 514 nm (1 mW/cm^2) for 5 min. Post-curing under normal white incandescent lamps was done for 5 min. The HPDLC samples were formed by interfering a split Argon-ion laser beam (514 nm) at an angle to form a Bragg spacing of 800 nm. The laser intensity (per beam) was 1 mW/cm^2 and the samples were exposed for 5 min. Samples were again post-cured for 5 min under an incandescent lamp.

For SEM analysis, the LC was extracted using methanol and the samples were mounted on appropriate SEM sample substrates. Prior to imaging, the samples were coated with 2–3 nm of tungsten to reduce charging. LVSEM images were taken with a Hitachi S-900 operating at 1 kV. Image analysis was performed using OPTIMAS [24], a software package in which a number of macros were written to analyze the SEM images. Micrographs taken with the S-900 were scanned at a high resolution and image analysis was performed on these images. The macros identified all domains (defined as dark areas in the micrographs) using thresholds input by the user. Once all objects were

Table 1
Calculated monomer functionalities based on HPLC results

Monomer	Effective functionality
A	4.8
B	4.0
C	3.8
D	3.2
E	2

Table 2
Summary of floodlit PDLC morphologies

Monomer	Average droplet diameter (nm)	Volume fraction (%)
A	10–40	15
B	10–40	12
C	10–40	11
D	10–40	9
E	N/A	0

identified, the program first generated an area fraction and then analyzed the data to yield average size and shape statistics. The macro was also programmed to fit each object so that the shape anisotropy of each domain could be obtained. For each domain, the length of the longest *x*-dimension (horizontal) and *y*-dimension (vertical) is defined by the OPTIMAS program. For a spherical object, the ratio of the longest *x* to *y*-measurement would be 1.0. If a domain shape was elliptical and the long axis of the domain was vertical, then the ratio would be less than 1.0. If the long axis of the domain was along the horizontal, then this ratio would be greater than 1.0. The program then generates an anisotropy ratio, *R*, by normalizing these *x*/*y* ratios around 0.0. A *R* value less than 0 indicates that the *y*-axes were larger than the *x*-axes, while a *R* value larger than 0 indicates that the *x*-axes were larger than the *y*-axes. The program generates a histogram of *R* values in which the shape of the curve and center point of the curves should be examined. If only spherical domains are formed (regardless of the size), then the histogram would contain a single value centered at $R = 0$ describing 100% of the data points. The spread of the actual data from this idealized delta function is related to the amount of observed variability in the associated shapes of the domains. For the grating samples, the images were rotated so that the grating vector was always parallel to the horizontal direction.

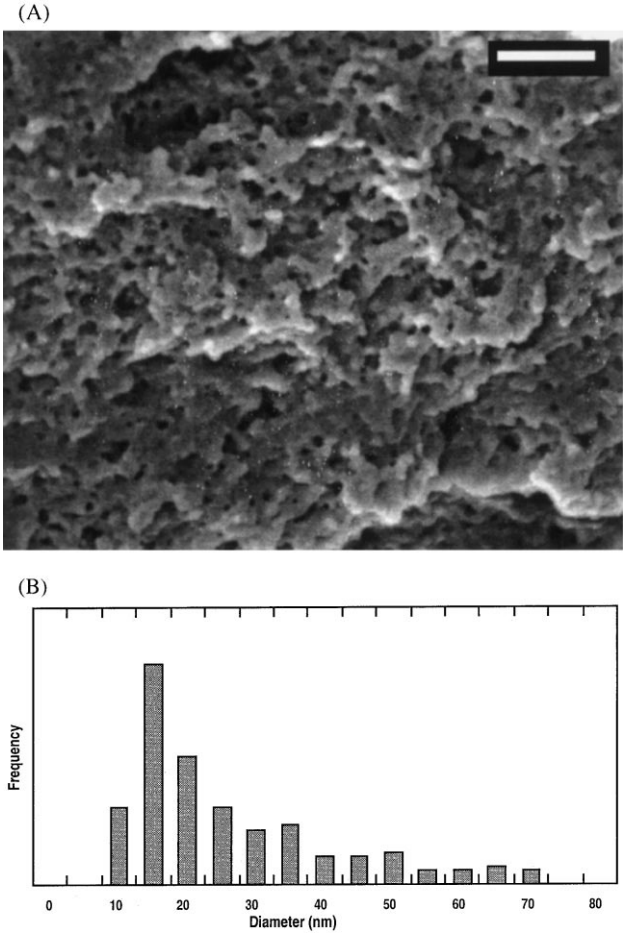

Fig. 3. LVSEM of flood-lit PDLC film prepared from monomer A where the scale bar equals 300 nm (A), and a histogram of domain diameters taken from flood-lit films formed from monomer A.

3. Results and discussion

Conventional floodlit samples were examined first, in order to suppress the effects of anisotropic diffusion on the resulting morphology. Fig. 3(A) shows the morphology of the PDLC sample fabricated from monomer A. A morphology resembling "Swiss cheese" is observed. This is the classic morphology typically associated with PDLCs. Discrete domains of LC are surrounded by polymer with little indication of any coalescence among the domains observed. However, note the scale bar on the micrograph. The largest domain is considerably less than 100 nm in diameter and the average size is closer to 20–30 nm in diameter. Fig. 3(B) shows a histogram of the average diameters from a large number of domains from this sample. The peak of the size distribution occurs at 15 nm and greater than 90% of the domains have diameters less than 50 nm. These sizes are not typically studied in conventional PDLC studies due to the samples' inherent lack of scattering. A volume fraction of 15% was measured (as shown in Table 2) indicating that a considerable LC fraction remained trapped in the matrix.

Droplets of this size indicate a phase separation mechanism in which very little droplet growth or coalescence occurs once discrete domains form. We speculate that discrete domain formation and "vitrification" occur almost simultaneously. This latter term, vitrification as used here, should be separated from the gelation point. In much previous literature on PDLC structure formation, the use of the terms gelation and vitrification are used

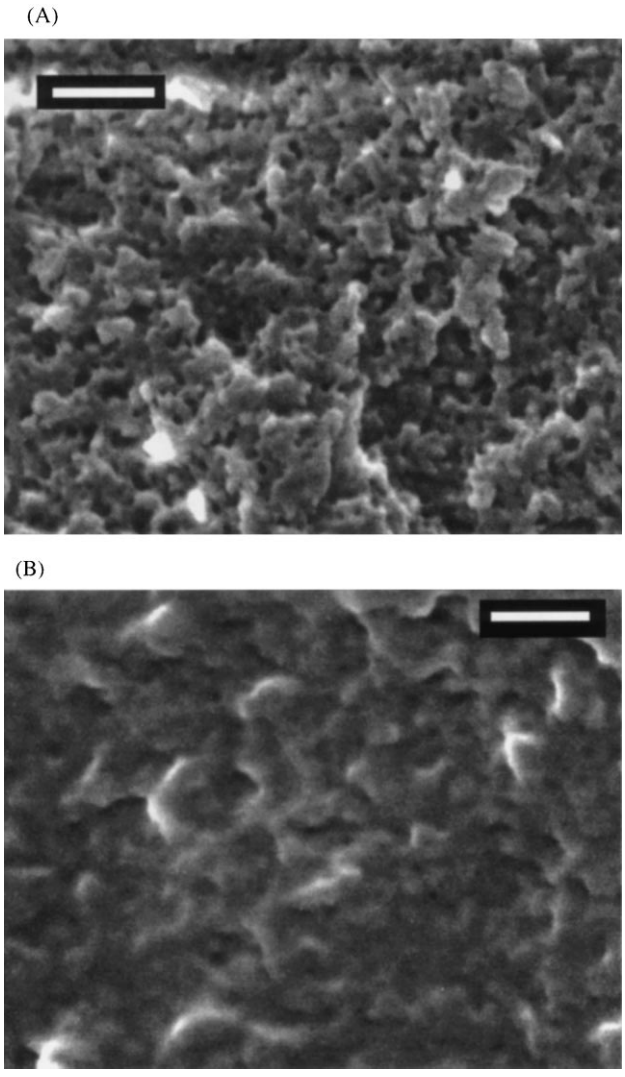

Fig. 4. LVSEM of flood-lit PDLC film prepared from (A) monomer C and (B) monomer E, wherein the scale bar equals 300 nm on both micrographs.

interchangeably, incorrectly. The high functionality of the monomers coupled with the fast reaction kinetics typical of free-radical reactions suggests that gelation (where conversion reaches >1% for multifunctional monomers [25] or where an infinite molecular cluster is formed) occurs very early in the reaction time frame. At this point in time, discrete domains of LC were not formed. As time progresses and the reaction proceeds, a point in time is reached wherein discrete domains form (assuming a nucleation and growth phenomena). In some instances, after this point the system has enough mobility to continue to change its inherent morphology until the viscosity of the system causes vitrification (or freezing of the structure). Thus, the terms gelation and vitrification are not the same when used in this context. The small domain sizes observed here strongly support the hypothesis that the formation of discrete domains and "vitrification" occur almost simultaneously thereby yielding very small LC domains with a high monodispersity of sizes. Once a domain form is formed, the growing polymer network essentially quenches all growth limiting the size distribution and further changes to the morphology. Real-time scattering data taken on similar floodlit systems indicate that the time to observe an onset of scatter typically associated with the occurrence of phase separation does not occur until a time greater than 1 min [26]. However, previous differential photo-calorimetry measurements [27] on similar systems at identical powers suggest that conversion reaches values >5% at times below 10 s. Thus, a comparison of the two time scales indicates that gelation occurred before the onset of phase separation.

As we reduce the functionality in these floodlit samples, several observations can be made. As shown in Fig. 4(A) and (B), a decrease in the amount of LC phase separated out is observed as indicated by the smaller volume fractions in Table 2. Monomer C, shown in Fig. 4(A) exhibits a similar LC domain size distribution as shown for monomer A in Fig. 3(B), but the amount of phase separated LC is reduced from 15 to 9%. For the monomer E sample, no phase separation is observed and the texture shown in Fig. 4(B) is attributed to glassy fracture of the polymer film. For all samples excluding E, very small LC domains were observed with a high degree of size monodispersity.

Observations generated from the detailed image analysis also reveal differences in the anisotropy of the domain shapes. Although the domains shown in Figs. 3(A) and 4(A) suggest nearly spherical domain sizes, a detailed analysis of many domains using the image software program indicates that anisotropic droplets are formed under these uniform illumination conditions. Fig. 5(A) and (B) show the anisotropy histograms taken from samples formed from monomers A and D. The data in Fig. 5(B) is closer to an ideal delta function than the data shown in Fig. 5(A). That is, much more of the data for monomer D is centered at R values near 0.0, while data taken from monomer A indicates larger excursions on both sides of $R = 0$. This larger breadth indicates considerably more variability in the average shape of the phase separated domains that was observed for the sample formed from the higher functionality syrup. The x-axis on both histograms run from -1 to $+1$ which would correspond to domains with twice as large y vs. x or x vs. y dimensions, respectively.

This data suggests two things: (1) as the functionality is increased, the driving force for phase separation is increased and that upon discrete domain formation; and (2) there are anisotropic stresses imparted onto the LC domains which are affected to some degree by the inherent functionality of the starting monomers. As the functionality is decreased, lower and lower volume fractions are observed up to the point where no phase separation takes place as observed with monomer E. The observation of very small LC domains coupled with the fact that there is no indication of coalescence and/or growth suggests that the formation of the LC domains occurs in a very short period of time and that this occurrence is essentially the end-point of the

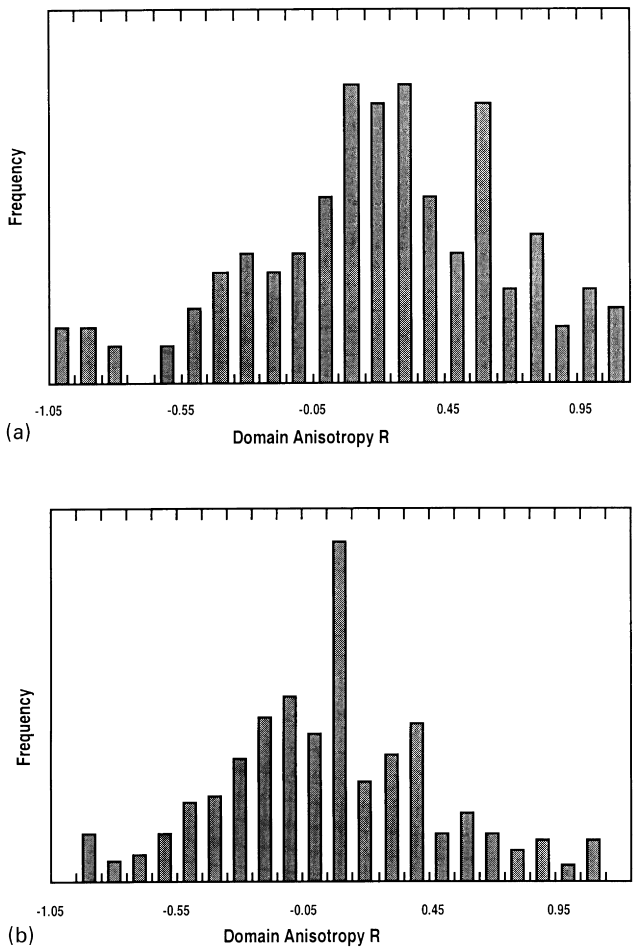

Fig. 5. Histogram of domain anisotropy in flood-lit PDLC films formed from (A) monomer A and (B) monomer D.

process. That is, little else happens once these small, highly monodisperse domains are formed. Based on previous arguments about gelation, we assume this domain formation happens in a cross-link rich environment (i.e. after gelation). Thus, it is reasonable to assume that the local environment the LC molecules 'feel' upon forming domains would be non-uniform due to the highly cross-linked nature of the polymer chains. Spherical LC domains would be expected in a network with low cross-link density and/or higher flexibility. The amount of stress experienced by the domain would be expected to decrease as the functionality was decreased. This speculation is confirmed by the trends indicated in droplet anisotropy. Although examining a different system on a different length scale, these results are qualitatively consistent with previously published work [20]. The lower the functionality of the syrup used, the weaker the driving force for phase separation, and thus lower volume fractions and less variability of the domain shapes were observed.

HPDLC samples were formed from all five of the monomers under identical conditions by interfering two beams on the sample in a transmission geometry. The

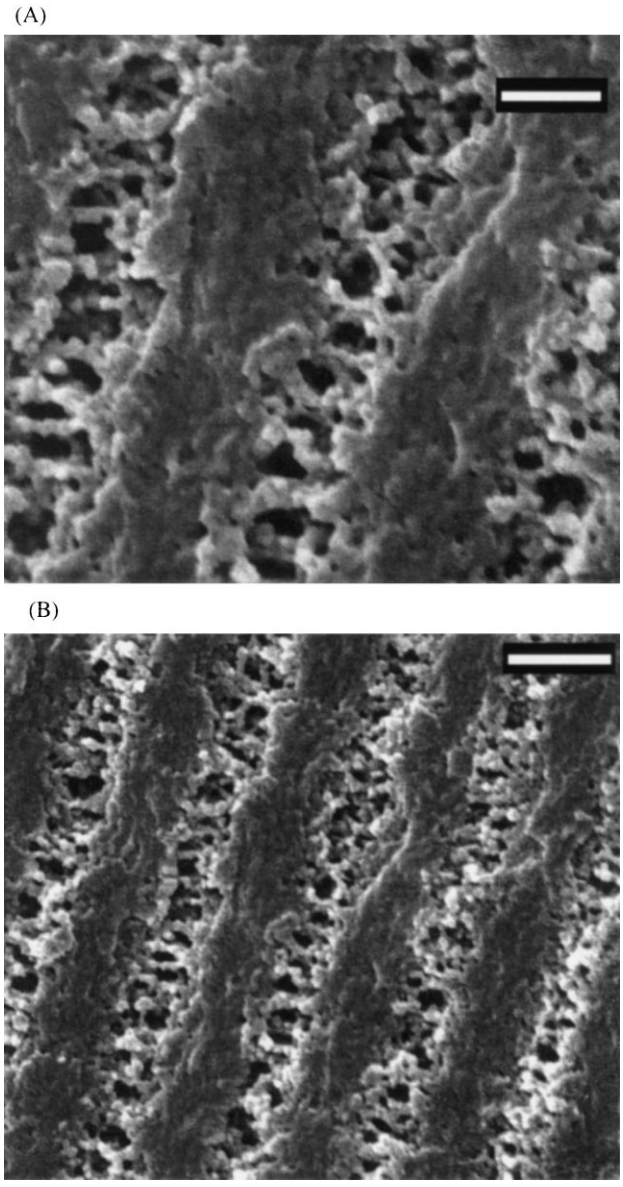

Fig. 6. High and low magnification LVSEM of HPDLC transmission grating prepared from monomer A, wherein the scale bar corresponds to (A) 300 and (B) 600 nm.

LVSEM micrographs of a 800 nm grating prepared from monomer A are presented in Fig. 6(A) and (B). There are several important distinctions between these micrographs and those taken from uniformly illuminated samples such as shown in Fig. 3(A). The grating microstructure consists of spatially-periodic domains separated by polymer walls rather than randomly placed domains as in the flood-lit case. The droplet sizes present in the LC-rich region are considerably larger in diameter and a much larger distribution of domain sizes is present. However, the size scale of these domains is still 1–2 orders of magnitude smaller than the conventional PDLC samples being explored for conventional scattering applications. At first glance, there appears to be considerably more anisotropy in the domain shapes as

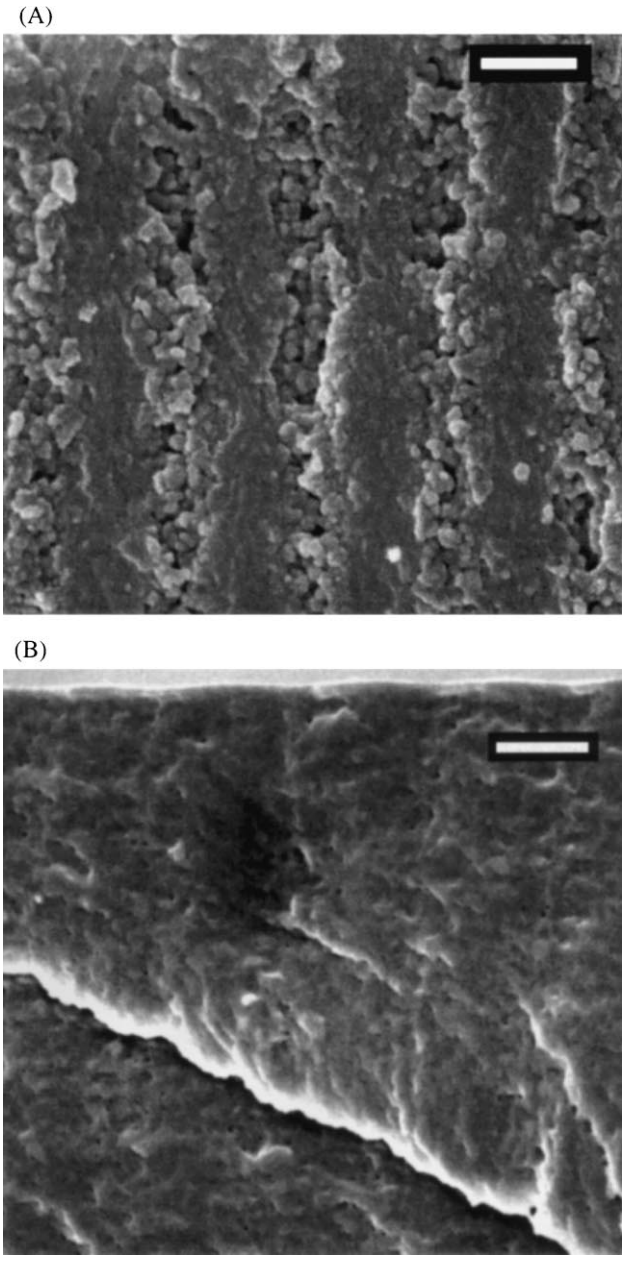

Fig. 7. LVSEM of HPDLC transmission gratings prepared from (A) monomer C and (B) monomer E, wherein the scale bar equals 600 nm on both micrographs.

compared to the floodlit samples. Furthermore, the droplet shape is preferentially parallel to the grating vector (perpendicular to the grating planes) for the sample shown in Fig. 6. There are considerably more LC domains in these micrographs than is observed for the flood-lit samples, although they are spatially segregated. For monomer A, approximately 50% of the LC-rich region is composed of domains while almost no phase separation of individual LC domains is observed in the polymer-rich regions. The fact that the local LC volume fraction is considerably higher than the initial LC loading (33% w/w), indicates that anisotropic diffusion of the LC takes place prior to phase separation in the grating samples.

Upon comparison to gratings prepared from monomers C and E (Fig. 7(A) and (B)), it is evident that the LC volume fraction decreases as the number of double bonds is decreased. The size of the LC domains also decreased. Table 3 summarizes the size of the droplets, the volume fractions and the LC/polymer ratio. This ratio describes the width of the LC-rich region with respect to the width of the polymer-rich region. It also indicates the relative contribution of each of these regions within a single grating spacing. Monomer E (Fig. 7(B)), similar to the floodlit samples, exhibits very few droplets indicating that most of the LC is trapped in the polymer matrix. The weak grating that can be observed in some micrographs is attributed to weak mechanical differences due to periodic mass density differences within the sample. An additional factor for monomer E may be the increased distance between cross-links leading to greater flexibility of the chain. In general, however, less and less of the LC phase separates out as the number of double bonds decreases. If one multiplies the local volume fraction to the LC ratio to give an indication of the global volume fraction (similar to what was measured in the flood-lit samples), a similar decrease in the amount of the LC is observed with respect to the number of double bonds as shown in Fig. 8. For a given initial loading of the LC, the diffusion of the LC induced by the interfering beams does not greatly effect the amount of total LC that is phase separated out until the higher functional monomers are used.

The same image analysis software was used to analyze the results from the grating samples and the results are shown in Figs. 9 and 10 from gratings of monomer A and D. Fig. 9 shows there is a considerable difference in the size and the dispersity of sizes of the LC domains for these two samples. Monomer A exhibits a larger spread in the size

Table 3
Summary of HPDLC transmission grating morphologies

Monomer	Droplet dimension (nm)	Local volume fraction (%)	LC/Polymer ratio
A	100–225	46	0.5
B	80–150	46	0.32
C	80–150	32	0.32
D	60–100	28	0.28
E	< 30	N/A	N/A

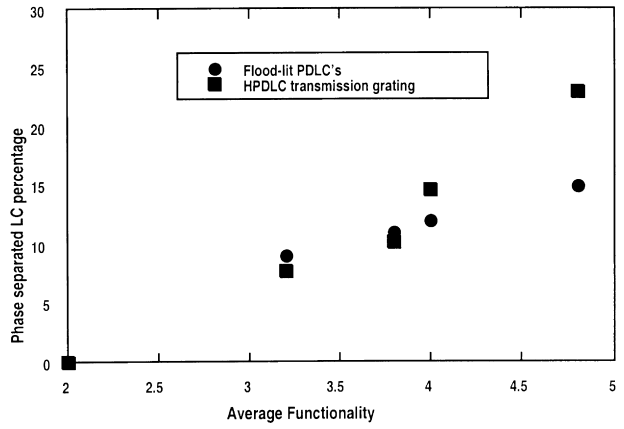

Fig. 8. Total volume fraction of phase separated LC for flood-lit and HPDLC films as a function of the starting monomer functionality.

distribution although most of the domains are less than 50 nm in diameter. The average size obtained for monomer D from Fig. 9(B) is slightly smaller, and by comparing the two cases one can see that monomer A has a substantially higher number of domains that are greater than 45 nm in diameter than monomer D. Fig. 10 is a comparison of the average anisotropy of the domain shapes. In this case, the sign of the R value (x-axis) is significant as positive values suggest anisotropy parallel to the grating plane (i.e. droplets shaped with long axis perpendicular to layer plane normals). Both Fig. 10(A) and (B) have an x-axis range of -1 to 2. For both cases, the peak of the distribution is centered at values larger than $R = 0$ confirming the visual inspection that there is significant shaping of the droplets due to anisotropic polymerization profile. The degree of shaping is larger for monomer A, however, as indicated by a greater shift in the peak of the distribution to larger R values and the much larger number of domains with positive R values as compared to monomer D. Compared to the histograms generated from the flood lit data, shown in Fig. 10, are considerably broader indicating more variability in the domain shapes.

Due to the spatial periodicity of the polymerization rates during grating formation, periodic forces rather than random thermal fluctuations drive the location of phase separation in the gratings. One can speculate that the distribution of cross-link density spatially across a grating period follows the overall trend as affected by monomer functionality. During

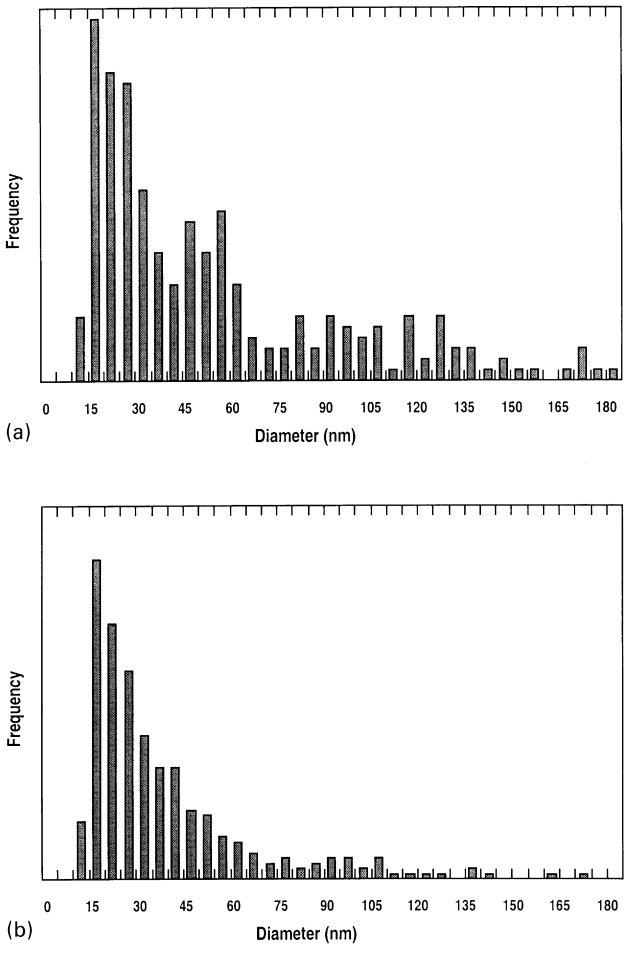

Fig. 9. Frequency of domain diameters for HPDLC films formed from (A) monomer A and (B) monomer D.

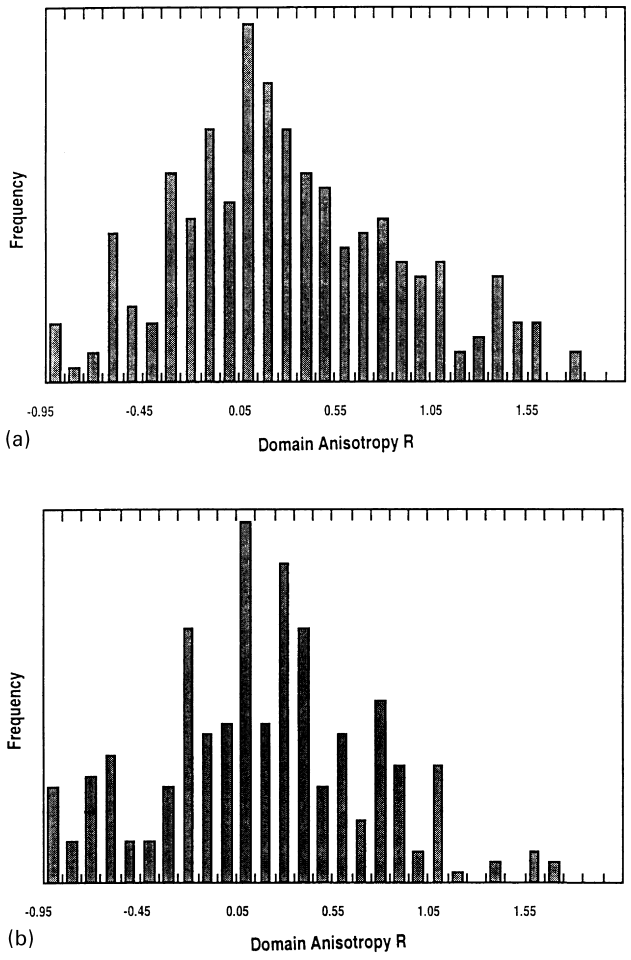

Fig. 10. Domain anisotropys for HPDLC films formed form (A) monomer A and (B) monomer D.

the formation of gratings, the LC diffuses from regions of high intensity illumination to regions of lower intensity illumination. A front of phase separating higher cross-linked density polymer lags behind the diffusing LC and at some time causes domain formation in the low intensity regions. Note, the polymer within these regions has already gelled but possesses a much lower cross-link density than the polymer in the high-intensity region. The onset of domain formation in the gratings occurs later in time relative to the flood-lit samples due to intensity arguments. The relative intensity a flood-lit sample observes is larger than the intensity the grating sample sees in the null of the interference pattern as the inherent intensity in these regions is lower. It is assumed, the conversion at the time of phase separation of the growing polymer chains would be higher in the grating films than in floodlit PDLCs. Higher conversions would lead to greater elastic forces on the droplet walls leading to the increase in percent phase separation and droplet anisotropy, both of which are experimentally observed. Such effects would be enhanced by the increased local LC concentration previously discussed. Thus, one would expect to see less LC phase separate out and that the domain anisotropy would be smaller as the number of double bonds in the monomer is decreased, both of which are observed experimentally.

4. Conclusion

Investigation of the effects of varying monomer functionality has been conducted in both floodlit PDLCs and holographic PDLC gratings. The results indicate that a decrease in the monomer functionality leads to decreased LC phase separation as indicated by lower volume fraction of the LC domains. Image analysis of both flood-lit and grating samples indicates considerably anisotropy in the observed domain shapes. This anisotropy is related to trends in the relative functionality of the starting syrups. Films formed from the higher functional monomers exhibit more variability in their domain shapes which is speculated to be due to differences in the local network environment. In the grating samples, the anisotropy is related to the direction of the gradient in intensity and this dependence decreases as functionality is decreased.

Acknowledgements

Partial financial support was provided by the Air Force Research Laboratory, Laser Hardened Materials Branch under contract F33615-95-C-5432 and through the DARPA Dual-Use Agreement F33615-97-2-5404. The authors would also like to thank Morley Stone and Michael Schulte for the HPLC analyses and D. Cleyrat Jr. for coding the OPTIMAS software and performing the image analysis.

References

[1] Drzaic PS. Liquid Crystal Dispersions. Singapore: World Scientific, 1995.
[2] Matsumoto S, Houlbert M, Hayashi T, Kubodera K-I. MRS Proc 1997;457:89.
[3] Matsumoto S, Houlbert M, Hayashi T, Kubodera K-I. Appl Phys Lett 1996;69:1044.
[4] Sansone MJ, Khanarian G, Leslie TM, Stiller M, Altman J, Elizondo P. J Appl Phys 1990;67:4253.
[5] Blacker RS, Lewis KL, Mason I, Sage I, Webb K. MRS Proc 1997;67:4253.
[6] Tanaka K, Kato K, Tsuru S, Sakai S. J SID 1994;2:37.
[7] Tanaka K, Kato K, Date M, Sakai S. SID Int Symp Dig Tech Papers 1995;26:267.
[8] Crawford GP, Fiske TG, Silverstein LD. SID Int Symp Dig Tech Papers 1996;27:99.
[9] Nelson EW, Williams AD, Crawford GP, Silverstein LD, Fiske TG. IST Proc 1997;50:673.
[10] Kitzerow HS. Mol Cryst Liq Cryst 1998;321:457.
[11] Fuh AY-G, Tsai M-S, Huang C-Y, Ko T-C, Chien L-C. Opt Quant Elect 1996;28:1535.
[12] Sutherland RL, Tondiglia VP, Natarajan LV, Bunning TJ. Chem Mat 1993;5:1533.
[13] Sutherland RL, Tondiglia VP, Natarajan LV, Bunning TJ, Adams WW. Appl Phys Lett 1994;64:1074.
[14] Bunning TJ, Natarajan LV, Tondiglia VP, Sutherland RL, Vezie DL, Adams WW. Polymer 1995;36:2699.
[15] Bunning TJ, Natarajan LV, Tondiglia VP, Sutherland RL. Mol Cryst Liq Cryst 1998;320:127.
[16] Sutherland RL, Tondiglia VP, Natarajan LV, Bunning TJ, Adams WW. SPIE Proc 1996;2689:158.
[17] Bunning TJ, Natarajan LV, Tondiglia VP, Dougherty G, Sutherland RL. J Polym Sci: Part B 1997;35: 2825.
[18] Bunning TJ, Natarajan LV, Tondiglia VP, Sutherland RL, Haaga R, Adams WW. SPIE Proc 1996;2651:44.
[19] Boots HMJ, Kloosterboer JG, Serbutoviez C, Touwslager FJ. Macromolecules 1996;29:7683.
[20] Serbutoviez C, Kloosterboer JG, Boots HMJ, Touwslager FJ. Macromolecules 1996;29:7690.
[21] Serbutoviez C, Kloosterboer JG, Boots HMJ, Paulisson FAMA, Touwslager FJ. Liq Cryst 1997;22:145.
[22] Dusek K. J Polym Sci: Part C 1967;16:1289.
[23] Dusek K, Prins W. Adv Polym Sci 1969;6:1.
[24] OPTIMAS 6, Optimas Corporation, 18911 Northcreek Parkway, Suite 101, Bothell, Washington, 98011, 206-402-8888.
[25] Kloosterboer JG. Adv Polym Sci 1988;84:1.
[26] T.J. Bunning, Unpublished data taken on similar systems with an increased LC concentration.
[27] Pogue RT, Bowman CN, Natarajan LV, Tondiglia VP, Sutherland RL, Bunning TJ. Polym Prep 1998;39:1024.